Analysis of the Impact of Sub-Hourly Unit Commitment on Power System Dynamics

T. Kërçi[a], J. Giraldo[b], F. Milano[a,*]

[a] *School of Electrical and Electronic Engineering, University College Dublin, Ireland*
[b] *Eindhoven University of Technology, Netherlands*

Abstract

This paper discusses the impact of the sub-hourly unit commitment problem on power system dynamics. Such an impact is evaluated by means of a co-simulation platform that embeds a sub-hourly stochastic mixed-integer linear programming security constrained unit commitment (sSCUC) into a time domain simulator, as well as includes a rolling planning horizon that accounts for forecast updates. The paper considers different sub-hourly sSCUC resolutions (i.e., 5 and 15 minutes) and different wind penetration levels (i.e., 25 and 50%). The focus is on the transient response of the system and on frequency variations following different sSCUC strategies, and different sSCUC wind power uncertainty and volatility. The case study consists of a comprehensive set of Monte Carlo simulations based on the 39-bus system.

Keywords: Co-simulation, dynamic performance, frequency stability, sub-hourly unit commitment, stochastic programming.

1. Introduction

Transmission system operators (TSOs) rely on hourly unit commitment (UC) models to economically operate the system [1]. Since large amounts of stochastic renewable energy sources (RES) can significantly impact on the performance of the system [2, 3], stochastic programming has been introduced in

*Corresponding author
Email addresses: taulant.kerci@ucdconnect.ie (T. Kërçi), federico.milano@ucd.ie (F. Milano)

recent years to properly account for uncertainty (e.g., wind) when scheduling the system [4]. For example, [5] shows that using a stochastic UC leads to decrease the operating cost and improve system performance. In [6], the authors show that a stochastic market-clearing procedure allows greater wind penetration compared to a deterministic approach.

A recent trend in the economic dispatch of power systems with high penetration of RES is the utilization of sub-hourly scheduling as opposed to the conventional hourly dispatch [7, 8]. This is what is currently happening in the European electricity market where more and more energy is being traded closer to real time (e.g., intraday) [9]. According to the European Electricity Balancing guideline [10], all EU countries should implement an Imbalance Settlement Period (ISP) of 15 minutes (i.e., switch from one hour to 15 minutes) by no later than Q4 2020. Likewise, the Australian Energy Market Operator (AEMO) is planning to use a 5 minute ISP by mid of 2021 [11].

The sub-hourly scheduling is a way to increase flexibility without investing in physical assets [12, 13]. In [14], it is shown that sub-hourly modeling allows to better capture the costs and the ramping capability of generators. In [15], it is shown that sub-hourly dispatch results in lower costs and lower reserves. The importance of sub-hourly modeling is also shown in [16], where the authors conclude that sub-hourly modeling reveal significant power plant cycling in the form of ramping and start-ups.

The works above study the impact of the sub-hourly modeling in power systems from the economic and/or operational point of view. The focus of our work, on the other hand, is on the impact of the sub-hourly UC on power system dynamics. If sub-hourly scheduling timescales are used, say 15-minute or 5-minute, in fact, then these timescales can overlap with long-term dynamics [17]. Therefore, it appears useful and timely to embed the UC problem into a fully-fledged transient stability analysis software tool [18, 19], and study the dynamic behaviour of power systems.

In the literature, this goal has been studied by including linear constraints into the UC formulation [20]. For example, [21] shows that, by including a

frequency ramp limit constraint (RoCoF) in the UC formulation, frequency is kept within its limits. Similarly, [22] shows that the inclusion of frequency constraints in the UC problem significantly affects UC decisions and lead to higher operating costs. The works above fail to capture the long-term frequency deviations of the system that are an important concern for system operators [23, 24].

Modern power systems embed different technologies such as communication networks, demand-side management, electric vehicles, and RES. Co-simulation is seen as a useful method to study the interactions of such complex systems [25]. This is due to the fact that a co-simulation approach allows the coupling of different subdomain models (e.g., power systems and electricity markets), where each subdomain is described and solved within its native environment without the need of simplifying one or another [26, 27]. For example, in [28] the authors propose a simulation platform that couples continuous power system simulators with discrete communication network simulators. In [29], a co-simulation method that couples electromagnetic transient and dynamic phasor simulations is proposed.

1.1. Contributions

The main contributions of this paper are the following:

- The development of a flexible co-simulation platform that allows evaluating the impact that different stochastic scenarios to model wind generation as well as different sub-hourly resolutions included in a UC problem have on power system dynamics.

- A comprehensive sensitivity analysis of the interaction between sub-hourly UC and power system dynamics based on Monte Carlo time domain simulations of stochastic differential-algebraic equations.

The proposed co-simulation platform is a tool aimed at helping TSOs to decide which UC problem (e.g., deterministic vs stochastic) is more adequate for their grid depending on the renewable penetration and the planning horizon. With

this aim, the paper compares various UC problem implementations with different approaches to handle uncertainty and volatility and discuss their impact on the long-term frequency deviations of the system.

1.2. Organization

The remainder of the paper is organized as follows. Section 2 describes the dynamic model of power systems based on stochastic differential algebraic equations (SDAEs); the modelling of stochastic processes; the mathematical formulation of the mixed-integer linear programming (MILP) stochastic security-constrained unit commitment (sSCUC); and the modelling of the sSCUC uncertainty and volatility, and rolling planning horizon. Section 2 also shows how the sSCUC and SDAEs interact together. The results of the case studies based on the IEEE 39-bus system are discussed in Section 3. Conclusions and future work are given in Section 4.

2. Modeling

2.1. Power system model

Power system dynamics with inclusion of stochastic processes can be modeled as a set of hybrid stochastic differential-algebraic equations (SDAEs) [30]:

$$\begin{aligned} \dot{\boldsymbol{x}} &= \boldsymbol{f}(\boldsymbol{x}, \boldsymbol{y}, \boldsymbol{u}, \boldsymbol{z}, \dot{\boldsymbol{\eta}}) \\ \mathbf{0} &= \boldsymbol{g}(\boldsymbol{x}, \boldsymbol{y}, \boldsymbol{u}, \boldsymbol{z}, \boldsymbol{\eta}) \\ \dot{\boldsymbol{\eta}} &= \boldsymbol{a}(\boldsymbol{x}, \boldsymbol{y}, \boldsymbol{\eta}) + \boldsymbol{b}(\boldsymbol{x}, \boldsymbol{y}, \boldsymbol{\eta})\, \boldsymbol{\xi} \ , \end{aligned} \tag{1}$$

where $\boldsymbol{f}$ are the differential equations; $\boldsymbol{g}$ are the algebraic equations; $\boldsymbol{x}$ are the state variables, e.g. generator rotor speeds; $\boldsymbol{y}$ are the algebraic variables, e.g. bus voltage angles; $\boldsymbol{u}$ are the inputs, e.g. load forecast and active power schedules; $\boldsymbol{z}$ are discrete variables, e.g. status of the machines); $\boldsymbol{\eta}$ represent stochastic perturbations, e.g. wind speed variations, which are modeled through the last term in (1); $\boldsymbol{a}$ and $\boldsymbol{b}$ represent the *drift* and *diffusion* of the stochastic differential equations (SDEs), respectively; and $\boldsymbol{\xi}$ represent the white noise vector.

Equations (1) are solved using numerical integration techniques for SDAEs. Since our analysis is based on long-term dynamic simulations, it is desirable that the model includes both electro-mechanical models and long-term dynamics models. In particular, (1) includes the dynamic models of synchronous machines, turbine governors (TGs), automatic voltage regulators, power system stabilizers, wind power plants, automatic generation control (AGC), and the discrete model of sSCUC. These are standard models used for transient stability analysis that are found, for example, in EuroStag and PSS/E software. TGs are modelled as a conventional droop (R) and a lead-lag transfer function, whereas the AGC is represented by an integrator with gain k_o. Wind power plants are represented by aggregated models, which implement a 5-th order Doubly-Fed Induction Generator (DFIG) with voltage, pitch angle and MPPT controllers [31].

2.2. Modelling of stochastic processes

Modelling the stochastic nature of wind power is critical in power system dynamic studies [32]. In this context, (1) includes only wind power variations with respect to the forecast wind generation as a stochastic perturbations. An Ornstein-Uhlenbeck Process (OUP) is used to model the stochastic nature of the wind speed v_s that enters into the wind turbine, as follows:

$$\begin{aligned} v_s(t) &= v_{s0} + \eta_v(t) \\ \dot{\eta}_v(t) &= \alpha_v(\mu_v - \eta_v(t)) + b_v\xi_v \end{aligned} \tag{2}$$

where v_{s0} is the wind speed initial value; η_v is the stochastic variable that is dependent on the drift $\alpha_v(\mu_v - \eta_v)$, and diffusion term b_v of the SDEs; α is the mean reversion speed that indicates the rate at which η_v tends to the mean value μ_v; and ξ_v represents the white noise.

2.3. Stochastic Unit Commitment Formulation

As the penetration of highly variable RES increases so does the uncertainty in power systems. This complicate the real-time balance between generation

and demand. Therefore it is of particular importance to model the uncertainty when scheduling the system. There are different methodologies and techniques proposed for optimization under uncertainty, with one of the most popular being the two-stage stochastic programming. In the context of UC, the two-stage stochastic UC makes use of a probabilistic model for the uncertain input parameters, e.g. wind generation, and is usually approximated by a set of scenarios representing the plausible realizations of these random parameters [4].

In this work, a standard MILP sSCUC problem is implemented based on [33], in which wind power production is considered as an uncertain parameter of the system, as follows:

$$\min_{H,W} \sum_{t\in\mathcal{T}}\sum_{g\in\mathcal{G}}(C_g^F z_{g,t}^F + C_g^{SU} z_{g,t}^{SU} + C_g^{SD} z_{g,t}^{SD}) \tag{3}$$
$$+ \sum_{\omega\in\Omega} \pi_\omega \left[\sum_{t\in\mathcal{T}}\sum_{l\in\mathcal{L}} C_g^V p_{g,t,\omega} + \sum_{t\in\mathcal{T}}\sum_{l\in\mathcal{L}} C^L L_{l,t,\omega}^{SH}\right]$$

such that

$$z_{g,t}^{SU} - z_{g,t}^{SD} = z_{g,t}^F - z_{g,t-1}^F \tag{4}$$
$$(\forall g \in \mathcal{G}, \forall t \in \{2..., T\})$$
$$z_{g,t}^{SU} - z_{g,t}^{SD} = z_{g,t}^F - IS_g \tag{5}$$
$$(\forall g, \forall t \in \{1\})$$
$$z_{g,t}^{SU} + z_{g,t}^{SD} \leq 1 \tag{6}$$
$$(\forall g, \forall t \in \{1..., T\})$$
$$z_{g,t}^F = IS_g \tag{7}$$
$$(L_g^{UP} + L_g^{DW} > 0, \forall g, \forall t \leq L_g^{UP} + L_g^{DW})$$

$$\sum_{\tau=t-UT_g+1}^{t} z_{g,\tau}^{SU} \leq z_{g,t}^{F} \tag{8}$$

$(\forall g, \forall t > L_g^{UP} + L_g^{DW})$

$$\sum_{\tau=t-DT_g+1}^{t} z_{g,\tau}^{SD} \leq 1 - z_{g,t}^{F} \tag{9}$$

$(\forall g, \forall t > L_g^{UP} + L_g^{DW})$

$$\sum_{g\in\mathcal{G}_n} p_{g,t,\omega} - \sum_{l\in\mathcal{L}_n} L_{l,t} + \sum_{l\in\mathcal{L}_n} L_{l,t,\omega}^{SH} + \sum_{f\in\mathcal{F}_n} W_{f,t,\omega} \tag{10}$$
$$- \sum_{f\in\mathcal{F}_n} W_{f,t,\omega}^{SP} = \sum_{m\in\mathcal{M}_n} \frac{(\delta_{n,t,\omega} - \delta_{m,t,\omega})}{X_{n,m}}$$

$(\forall n, \forall t, \forall \omega \in \Omega)$

$$p_{g,t,\omega} \leq P_g^{\max} z_{g,t}^{F} \tag{11}$$

$(\forall g, \forall t, \forall \omega \in \Omega)$

$$p_{g,t,\omega} \geq P_g^{\min} z_{g,t}^{F} \tag{12}$$

$(\forall g, \forall t, \forall \omega \in \Omega)$

$$p_{g,t,\omega} \leq (P_g^{IS} + RU_g) z_{g,t}^{F} \tag{13}$$

$(\forall g, \forall t \in \{1\}, \forall \omega \in \Omega)$

$$p_{g,t,\omega} \geq (P_g^{IS} - RD_g) z_{g,t}^{F} \tag{14}$$

$(\forall g, \forall t \in \{1\}, \forall \omega \in \Omega)$

$$p_{g,t,\omega} - p_{g,t-1,\omega} \leq (2 - z_{g,t-1}^{F} - z_{g,t}^{F}) P_g^{SU} \tag{15}$$
$$+ (1 + z_{g,t-1}^{F} - z_{g,t}^{F}) RU_g)$$

$(\forall g, \forall t \in \{2, ..., T\}, \forall \omega \in \Omega)$

$$p_{g,t-1,\omega} - p_{g,t,\omega} \leq (2 - z_{g,t-1}^{F} - z_{g,t}^{F}) P_g^{SD} \tag{16}$$
$$+ (1 - z_{g,t-1}^{F} + z_{g,t}^{F}) RD_g)$$

$(\forall g, \forall t \in \{2, ..., T\}, \forall \omega \in \Omega)$

$$L_{l,t,\omega}^{SH} \leq L_{l,t} \tag{17}$$

$(\forall l, \forall t, \forall \omega \in \Omega)$

$$W_{f,t,\omega}^{SP} \leq W_{f,t,\omega} \tag{18}$$

$(\forall f, \forall t, \forall \omega \in \Omega)$

$$-P_{n,m}^{\max} \leq \frac{(\delta_{n,t,\omega} - \delta_{m,t,\omega})}{X_{n,m}} \leq P_{n,m}^{\max} \tag{19}$$

$$(\forall n, m \in M_n, \forall t, \forall \omega \in \Omega)$$

$$p_{g,t,\omega}, L_{l,t,\omega}^{SH}, W_{f,t,\omega}^{SP} \geq 0 \tag{20}$$

$$(\forall g, \forall l, \forall f, \forall t, \forall \omega \in \Omega)$$

$$z_{g,t}^{F}, z_{g,t}^{SU}, z_{g,t}^{SD} \in \{0, 1\} \tag{21}$$

$$(\forall g, \forall t)$$

and the initial state conditions are as follows:

$$IS_g = \begin{cases} 1 & \text{if } ON_g > 0 \\ 0 & \text{if } ON_g = 0 \end{cases}$$

$$L_g^{UP} = \min\{T, (UT_g - ON_g)IS_g\}$$

$$L_g^{DW} = \min\{T, (DT_g - OFF_g)(1 - IS_g)\}$$

Equations (3) represent the total cost to be minimized which includes the fixed, start-up, shut-down and variable cost of the generating units, as well as the cost of involuntarily demand curtailment. Equations (4)-(6) model the logical expression between the binary variables (i.e., start-up and shut-down of generating units). Equations (7)-(9) model the minimum and maximum up- and down-time constraints. The power balance constraint is modeled through equations (10). While the capacity limits of generating units are modeled through equations (11)-(12) and their respective ramping limits through (13)-(16). Equations (17)-(18) model the limits of the involuntary demand curtailment and wind power spillage, respectively. Transmission capacity limits are enforced by equations (19). Finally, equations (20)-(21) refer to the variable declarations.

The model shown in (3)-(21) is the deterministic equivalent of the original two-stage stochastic programming problem. It is called a two-stage problem since there are first-stage and second-stage variables, also known as here-and-now and wait-and-see variables, respectively [4]. In particular, $z_{g,t}^{F}, z_{g,t}^{SU}, z_{g,t}^{SD}$ are first-stage decision variables that represent the status of generating unit g

in time period t (i.e., ON/OFF status, start-up and shut-down). These decisions do not depend on uncertainty realization ω, and are generally made one day in advance. Similarly, $p_{g,t,\omega}, L^{SH}_{l,t,\omega}, W^{SP}_{f,t,\omega}, \delta_{n,t,\omega}$ are second-stage decision variables that represent the active power dispatch of generating units g in time period t and scenario ω, the involuntary power curtailment from load l in time period t and scenario ω, wind power spillage from wind production unit f in time period t and scenario ω, and voltage angle at node n in time period t and scenario ω, respectively. All second-stage decision variables depend on uncertainty realization ω. Further details of the sSCUC can be found in [33] and references therein.

2.4. Scenarios and Rolling Horizon within the sSCUC

To illustrate the modelling of sSCUC wind uncertainty and volatility, and rolling planning horizon used in this paper, we show below the power balance equations of the sSCUC, as follows:

$$\sum_{g\in\Omega_{\mathrm{G_n}}} p_{g,t,\omega} - \sum_{l\in\Omega_{\mathrm{L_n}}} L_{l,t} + \sum_{l\in\Omega_{\mathrm{L_n}}} L^{SH}_{l,t,\omega} + \sum_{k\in\Omega_{\mathrm{K_n}}} W_{k,t,\omega} - \sum_{k\in\Omega_{\mathrm{K_n}}} W^{SP}_{k,t,\omega} = \sum_{m\in\Omega_{\mathrm{M_n}}} \frac{(\delta_{n,t,\omega} - \delta_{m,t,\omega})}{X_{n,m}}, (\forall n, \forall t, \forall \omega \in \Omega) \tag{22}$$

where $p_{g,t,\omega}$ is the active power of conventional generating units g, at time period t, and scenario ω (i.e., equivalent of the second-stage variable $u_{f,t,\omega}$ in section 2.3); $L_{l,t}$ is the demand for load l at time period t; $L^{SH}_{l,t,\omega}$ is the power curtailment from load l, at time period t, and in scenario ω; $W_{k,t,\omega}$ and $W^{SP}_{k,t,\omega}$ represent the power generation and curtailment, respectively, from wind unit k, in time period t, and scenario ω; $X_{n,m}$ is the reactance of line $n-m$; $\delta_{n,t,\omega}$ represent the voltage angle at node n, time period t, and scenario ω; and $\Omega_{\mathrm{K_n}}$, $\Omega_{\mathrm{M_n}}$ are the sets of stochastic power generation (i.e., wind) located at node n, and nodes $m \in N$ connected to node n by transmission line, respectively.

2.4.1. Modelling wind uncertainty

Similar to [34], a wind power penetration level $W_{k,t,\omega}$ is defined as a percentage of the demand $L_{l,t}$, and named the medium scenario, $W^{M}_{k,t,\omega}$. Then,

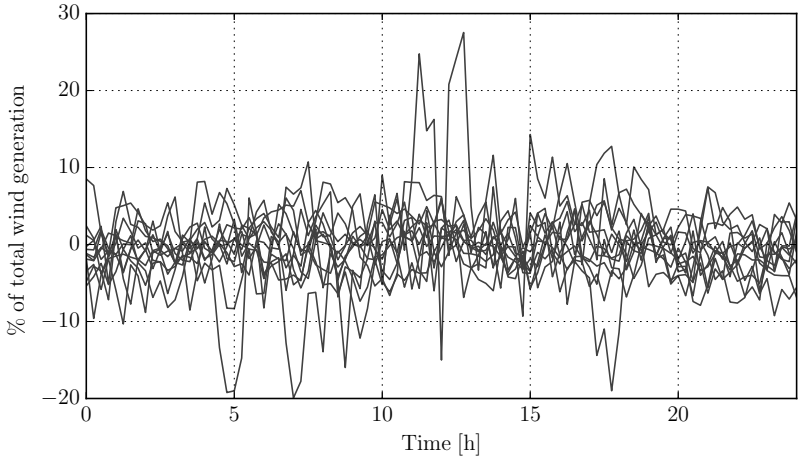

Figure 1: Wind power 15min rate of change for 12 typical day in the Irish system in 2018.

high and low wind power scenarios ($W^H_{k,t,\omega}, W^L_{k,t,\omega}$) are built as percentages of the medium scenario, as follows:

$$\begin{aligned} W^L_{k,t,\omega} &= W^M_{k,t,\omega} \times (1 - j/100) \\ W^H_{k,t,\omega} &= W^M_{k,t,\omega} \times (1 + j/100) \end{aligned} \tag{23}$$

where j is the percentage of deviation of the the high and low scenarios with respect to the medium one.

The consistency of the wind power scenarios with real-world information is compared using wind power data of the Irish system[35]. Specifically, the 15 minute rate of change of wind power is determined based on one typical day per each month of 2018 (see Fig. 1). Based on these data, wind power does not appear to be able to change more than 10% in 15 minutes. For this reason, in the case study, $j = 10\%$ is assumed.

2.4.2. Modelling wind volatility

Wind power volatility is modelled as small fluctuations with respect to the average value for a given period. Hence, uncertainty is related to wind power forecast, e.g. wind scenarios, while volatility is considered as a percentage,

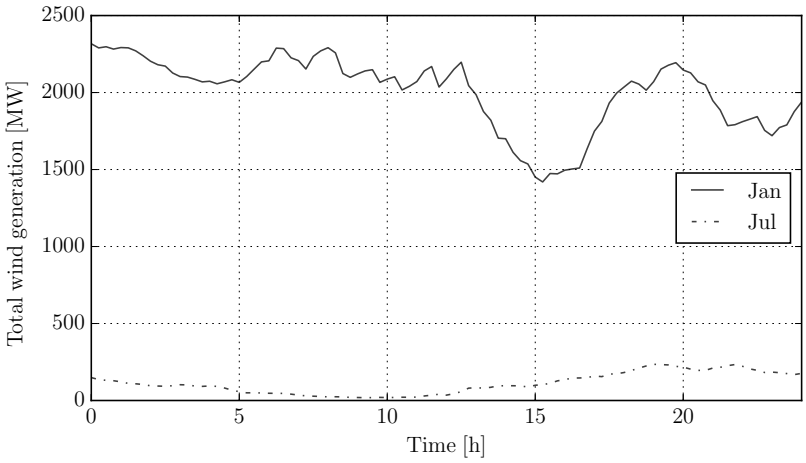

Figure 2: Wind power profile for two typical days (Jan, Jul) in the Irish system in 2018.

e.g. standard deviation, on top of the wind power forecast [36]. A normal distribution $N(\mu, \sigma^2)$ with zero mean and given standard deviation is attached to each wind power scenario, as follows:

$$\begin{aligned} W^{L1}_{k,t,\omega} &= W^{L}_{k,t,\omega} + N(0, \sigma^2) \\ W^{M1}_{k,t,\omega} &= W^{M}_{k,t,\omega} + N(0, \sigma^2) \\ W^{H1}_{k,t,\omega} &= W^{H}_{k,t,\omega} + N(0, \sigma^2) \end{aligned} \tag{24}$$

where $W^{L1}_{k,t,\omega}, W^{M1}_{k,t,\omega}, W^{H1}_{k,t,\omega}$ are the new low, medium and high wind power scenarios, respectively, after adding the volatility.

An important aspect to keep in mind when building the scenarios is the relationship between the wind power level and its standard deviation σ. With this aim, two typical days are analysed for two months, namely January (high wind) and July (low wind). The wind power profile for these typical days is shown in Fig. 2. It appears that wind varies more in January than in July. More specifically, the standard deviation of wind power generation is found to be 234.78 MW and 68.46 MW, for January and July, respectively, and that high wind leads to higher σ.

Note that the goal is not to propose new sSCUC models to deal with wind

power uncertainty and volatility, but rather to study the impact of a well assessed sSCUC formulation on power system dynamics. For this reason, it is not necessary to consider more sophisticated sSCUC models. As a matter of fact, the case study shows that, depending on the wind penetration and planning horizon, a sSCUC might not be needed at all.

2.4.3. Modelling the rolling planning horizon

Scheduling the system frequently (i.e., more than once a day) allows having better wind and load forecats. As a result, less reserves are required [5]. In this work, we use a rolling planning approach for updating the wind power forecast ($W_{k,t,\omega}$) with a planning horizon of 24h. During the first hour of the planning horizon, the high/low wind scenarios increase/decrease as a linear function from the medium scenario and after that they have a fixed error, e.g. $j = 10\%$. The sSCUC model is solved at every time period t during the first 12h with a planning horizon of 24h. When rolling forward, the status of the units of the previous horizon serve as an initial status for the next horizon. Between two scheduling events of the sSCUC, e.g. 15 or 5 minutes, wind and load profiles are modelled as linear ramps.

2.5. Interaction between sSCUC and SDAEs

It is time to merge all of the above in a single framework. Generally speaking, the goal is to embed equations (3)-(21) and (23)-(24) into equations (1). One has two ways to do so: embed sSCUC and equations (23)-(24) into an existing dynamic model, or the other way round. This paper proposes the former approach, i.e., embedding the sSCUC problem (3)-(21) and equations (23)-(24) into the TDS routine of DOME [37].

The sSCUC model (3)-(21) uses the active power of the generators, namely, $p_{g,t,\omega}$, as a second-stage decision variable. In other words, $p_{g,t,\omega}$ adapts to the uncertainty realization ω. Since we are interested in having a single power dispatch for each generator and for each time period, a reasonable tradeoff consists in taking a weighted-sum of the scenarios ω. In the literature, one

may find different formulations of sSCUC with respect to the active power of generators. For example, in [38], the authors use the active power as a first-stage decision variable ($p_{g,t}$, set-points) and then use up/down reserve deployment (production changes) as a second-stage decision variable to accommodate wind variability (real-time).

Figure 3 shows the overall structure of the recently proposed co-simulation framework. The tool is composed of two parts, namely, the dynamic model of power systems (SDAEs) and the discrete model of sSCUC. DOME coordinates the co-simulation, i.e., the exchange of information between the sSCUC and the SDAEs. In particular, the output of the sSCUC model, namely, the active power of generating units, $p_{g,t,\omega}$, serves as an input to the SDAEs, i.e. change the power set point of the turbine governors of the power plants. Finally, a Monte Carlo method is utilized to simulate large sets of realizations of the stochastic processes of wind and loads. Each realization defines the "reality" that needs to be updated to solve the next sSCUC problem. Such a feedback is needed to update the forecast of wind ($W_{k,t,\omega}$) and loads as utilized in the sSCUC problem.

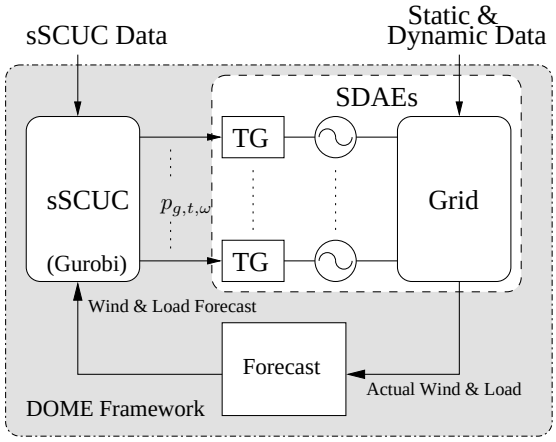

Figure 3: Interaction between the sSCUC problem and the dynamic model of the turbine governors, the synchronous machines and the grid.

3. Case studies

From a system operator point of view, it is useful to study the impact that different levels of uncertainty and volatility, e.g. wind forecast errors, within the sSCUC model have on power system dynamic performance. Since TSOs still mostly rely on deterministic security-constrained UC (SCUC) formulations, a comparison between SCUC and sSCUC approaches is relevant. Also, since different TSOs use different scheduling timescales and/or different rolling approaches, e.g. every 15 minute [39], or every 5 minute [8], a comparison of the effect of these strategies is also carried out in this section. Moreover, the impact of contingency and renewable penetration on the transient response of the system and long-term frequency deviations, respectively, using different sSCUC strategies is shown as well. Finally, the impact of different wind power scenarios of the sSCUC on the dynamic response of the system is discussed.

All simulations are based on a modified IEEE 39-bus system [40], with the data of the sSCUC taken from [41]. Whereas the value of load curtailment is assumed \$1000/MWh [4], and the marginal cost of wind is considered zero. The focus is on the first 12 hours of the planning horizon. During these hours the demand increases from 700 MW in the first hour to 1500 MW in the 12 hour. For simplicity, a wind profile that follows the demand is modelled. In other words, we assume the same wind penetration level for the medium scenario during these hours, namely, 25%, and based on this we build the low and high scenario accordingly. Such a relationship between demand and wind power corresponds to a typical day in 2018 in the Irish system. It should be noted here that one may choose any other profile for the demand and wind but according to our studies that does not change the relevant conclusions. Wind generation is given by three wind power plants connected at bus 20, 21 and 23, respectively, with a nominal capacity of 300 MW each.

The total number of state and algebraic variables of the SDAE model for all scenarios are 173 and 277, respectively. Regarding the sSCUC variables, the model includes three first-stage variables, namely, the ON/OFF, start-up and

shut-down status of generating units, and four second-stage variables, namely, the active power of conventional units (set-points), the demand and wind power curtailment, and the bus voltage angle, respectively. The total numbers of the first-stage and second-stage variables for the 15-minute model are 2,880 and 20,448, respectively. While the total numbers of these variables for the 5 minute model are 8,640 and 61,344, respectively. Therefore even considering only three wind power scenarios, shortening the time period of sSCUC, lead to a huge increase in the size of the sSCUC model. In fact, this is one of the main limitations of sSCUC approaches, especially when considering their use for real-time operations of power systems.

Finally, a Monte Carlo method is used in all scenarios (100 simulations are solved for each scenario). The standard deviation of the frequency of the COI, σ_{COI}, (computed as the average of the standard deviation obtained for each trajectory) is utilized as an index to evaluate the impact of sSCUC on the dynamic response of the system. The sSCUC is implemented in the Python language and solved using Gurobi [42], while all simulations are obtained using DOME, a Python-based software tool [37]. DOME includes a set of dynamic models similar to the ones provided by commercial software tools but with the additional feature of being able to model and properly integrate stochastic processes.

3.1. 15-Minute Scheduling

In this case study, a 15-minute scheduling time period is used. The average value of the objective function is found to be approximately $412,000, hence, lower than the value found in, for example, [41]. This is due to the fact that wind generation is explicitly accounted in the objective function, and since its marginal production cost is considered zero, it leads to lower operational costs. Each scenario is characterized by a relevant amount of wind stochastic variations. When solving the sensitivity analysis, the sSCUC probabilities are varied, and their impact on the standard deviation of the frequency of the system (σ_{COI}) is observed.

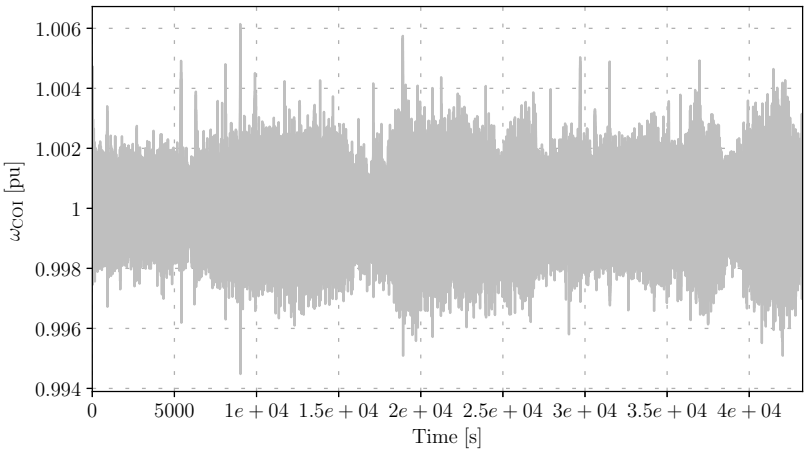

Figure 4: 15-minute scheduling – Trajectories of ω_{COI} for 12h.

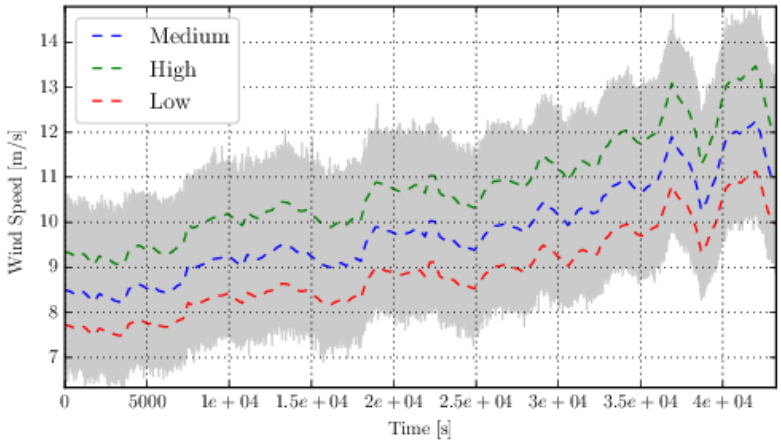

Figure 5: 15-minute scheduling – Trajectories of wind speeds for 12h. Dashed lines indicate the high, medium and low scenarios, respectively, while grey line indicate the same scenarios with inclusion of volatility.

In order to compare results, a base-case scenario is considered with the following properties: sSCUC probabilities for the low, medium and high wind power scenarios are set to 20%, 60%, 20%, respectively. Similarly, when we

run the Monte Carlo TDS (MC-TDS), the system is assumed to be with the following probabilities: 20%, 60%, 20% for the low, medium and high wind power scenario, respectively. As mentioned in the rolling planning section, the low and high scenario differ from the medium scenario by 10%. This base case is shown in Fig. 4, 5, while Fig. 4 shows the trajectories of ω_{COI} and Fig. 5 shows the trajectories of the wind speed scenarios.

It is interesting to note that, in Fig. 4, the frequency jumps due to a change in the operating point of the machines forced by the sSCUC, i.e. new schedules. These jumps are very similar to real-world power systems behaviour observed in, for example, the continental European grid [24, 43]. Finally, it is worth mentioning that the wind speed profile in Fig. 5 is obtained by adding some stochastic noise on each of the three wind scenarios.

3.1.1. Impact of different sSCUC strategies on power system dynamics

Table 1 shows some of the most relevant results of the sensitivity analysis. Specifically, scenario 1 assumes a sSCUC with wind probabilities 20%, 60%, 20% and a MC-TDS with the same probabilities. Thus, it is assumed that what was forecast by the sSCUC will actually happen in the reality. σ_{COI} for this scenario is 0.000847. In Scenario 2 the probabilities of the sSCUC differ from that of the system by a relevant value. The value of σ_{COI} is 0.000859, and thus higher than scenario 1 due to the error in the sSCUC probabilities.

Scenario 3 assumes a sSCUC with 100% low wind (one scenario, equivalent to SCUC). The value of σ_{COI} for this scenario is 0.000867 and so higher than scenario 1 for the same reason above. Similarly, Scenario 4 assumes a sSCUC with 100% medium wind. This leads to higher frequency variations compared to scenario 1, with $\sigma_{\mathrm{COI}} = 0.000872$. Next, Scenario 5 assumes a sSCUC with 100% high wind. Quite surprisingly this scenario appears to be the best from the dynamic point of view with $\sigma_{\mathrm{COI}} = 0.000802$.

To analyse this relevant case, more scenarios are considered. In Scenarios 6 to 9 in Table 1, the probabilities of sSCUC are varied from a sSCUC with 100% high wind to a sSCUC with 100% medium, and it can be seen that σ_{COI}

Table 1: 15-minute scheduling – σ_{COI} for different sSCUC probabilities with $j = 10\%$.

Scenario	sSCUC	MC – TDS	σ_{COI} (10^{-4})
1	20% 60% 20%	20% 60% 20%	8.47
2	40% 50% 10%	20% 60% 20%	8.59
3	100% 0% 0%	20% 60% 20%	8.67
4	0% 100% 0%	20% 60% 20%	8.72
5	0% 0% 100%	20% 60% 20%	8.02
6	0% 20% 80%	20% 60% 20%	8.17
7	0% 40% 60%	20% 60% 20%	8.32
8	0% 60% 40%	20% 60% 20%	8.41
9	0% 80% 20%	20% 60% 20%	8.52

increases almost linearly. Therefore, even though Scenario 5 assumes an error in the sSCUC probabilities, synchronous machines and the respective controls (primary and secondary) can regulate it very fast.

To further analyse this, in Table 2 the wind power uncertainty level is increased from $j = 10\%$ to $j = 30\%$ with a step of 10% for both, Scenario 1 and Scenario 5, respectively. For $j \geq 30\%$, Scenario 1 gives the better dynamic behaviour. It appears that, if the wind forecast error is small, then from the dynamic performance viewpoint of the system, it is better to solve a SCUC with high wind power.

It is worth observing that the differences on the long-term frequency deviations of the system between scenarios are marginal (maximum of 3.5 mHz). This is mainly due to the fact that, since the scheduling is repeated with a short period, it reduces the forecast error, which in turn leads different sSCUC strategies to produce similar schedules for the generators. This indicates that system operators may prefer to use deterministic approaches when scheduling

Table 2: 15-minute scheduling – σ_{COI} for different sSCUC probabilities and different j.

Scenario	j	sSCUC	MC – TDS	σ_{COI} (10^{-4})
1	10%	20% 60% 20%	20% 60% 20%	8.47
1	20%	20% 60% 20%	20% 60% 20%	12.58
1	30%	20% 60% 20%	20% 60% 20%	17.20
5	10%	0% 0% 100%	20% 60% 20%	8.02
5	20%	0% 0% 100%	20% 60% 20%	12.41
5	30%	0% 0% 100%	20% 60% 20%	17.37

Table 3: 15-minute scheduling – σ_{COI} for different sSCUC probabilities with $j = 10\%$.

Scenario	sSCUC	MC – TDS	σ_{COI} (10^{-4})
1	0% 0% 100%	0% 0% 100%	8.01
2	0% 100% 0%	0% 100% 0%	2.90
3	100% 0% 0%	100% 0% 0%	1.46

the system as the complexity of the stochastic one does not provide a solution with a significant added value for the operation of the system.

Finally, Table 3 compares three deterministic cases, namely, low, medium and high sSCUC wind power scenarios. The deterministic low wind power scenario leads to better dynamic behaviour (lower σ_{COI}).

3.1.2. Impact of sSCUC wind uncertainty on power system dynamics

To simulate the impact of the sSCUC wind power uncertainty, the uncertainty level is increased from $j = 10\%$ to $j = 40\%$ with a step of 10% (volatility is kept constant). Four σ_{COI} are calculated and Fig. 6 shows σ_{COI} as a function of wind power uncertainty. The higher wind uncertainty, the higher σ_{COI}. This relationship is almost linear within the used range. This suggests that as power

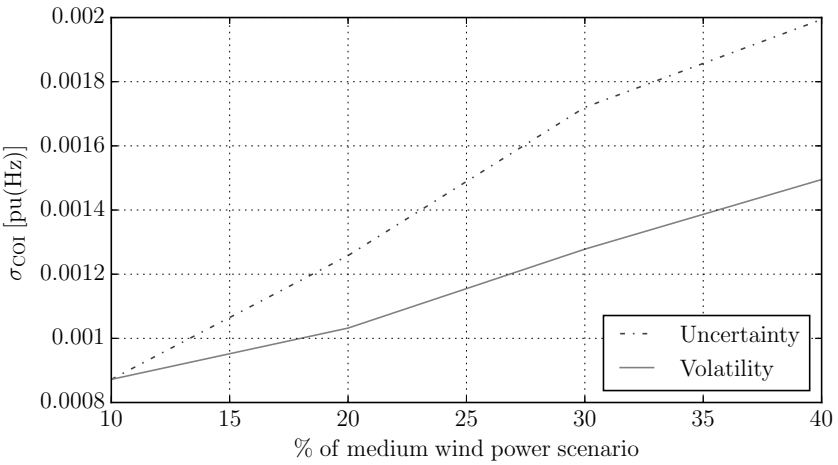

Figure 6: 15-minute scheduling – σ_{COI} as a function of wind uncertainty and volatility.

systems accommodate larger amounts of RES, i.e. higher uncertainty, TSOs will have to make sure that they have the necessary sources (power reserve) to cope with this uncertainty.

Figure 7 shows the total cost as a function of wind uncertainty. The higher the wind uncertainty, the higher the cost due to more ramp-up and ramp-down of generators. Hence, despite RES being a cheap source of energy, their intermittent nature, requires more reserves to cope and so there will be an increase of the cost of ancillary service. These results confirm the conclusions of previous works, e.g. [34].

3.1.3. Impact of sSCUC wind volatility on power system dynamics

To study the impact of sSCUC wind power volatility on power system dynamics, different level of volatility are considered, i.e., higher standard deviations means high wind volatility. The standard deviation of wind scenarios is increased from 10% to 40% with a step of 10% while uncertainty is kept constant.

Figure 6 shows σ_{COI} as a function of wind power standard deviation. The higher the wind power volatility, the higher the frequency variations. Similarly

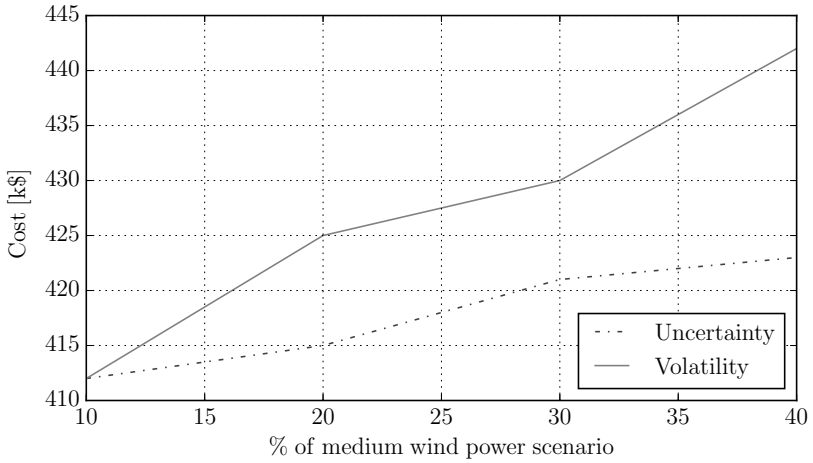

Figure 7: 15-minute scheduling – Expected cost as a function of wind uncertainty and volatility.

to the results shown in Fig. 6, this relationship appears to be almost linear within the considered range. As mentioned above, this supports the idea for increased ancillary services by TSOs in the future.

Figure 7 shows the total cost as a function of wind volatility where it can be seen that higher wind power volatility leads to higher costs due to higher ramping of generating units. Wind power volatility has thus a greater impact than uncertainty on costs.

3.2. 5-Minute Scheduling

In this scenario, the wind power uncertainty level is assumed proportional lower compared to the 15-minute scheduling time period ($j = 3.33\%$). This assumption is made based on the 15-minute rate of change of wind power shown above (Fig. 1). Next, the base case scenario is depicted in Fig. 8, 9. Compared to the base-case scenario in the 15-minute case study (Fig. 4), frequency variations are lower (Fig. 8). Also, it is interesting to note that high frequency variations correspond to the wind ramp-up. Regarding the total operating cost, its average value is found to be approximately \$408,000, and hence, lower than in 15-minute case study due to lower uncertainty.

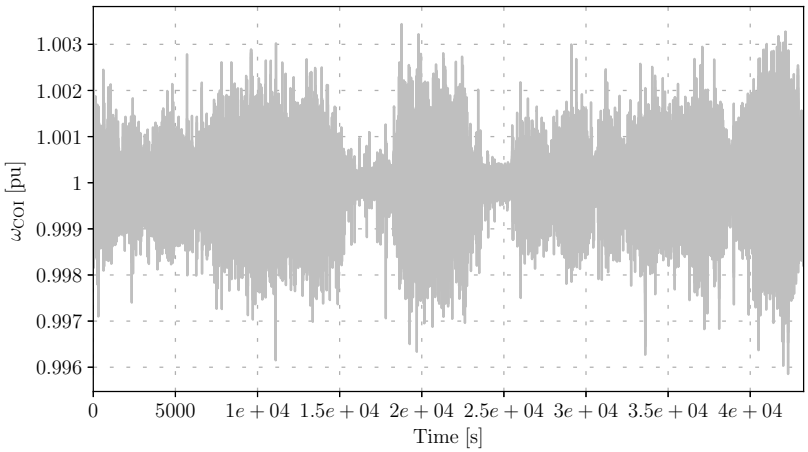

Figure 8: 5-minute scheduling – Trajectories of ω_{COI} for 12h.

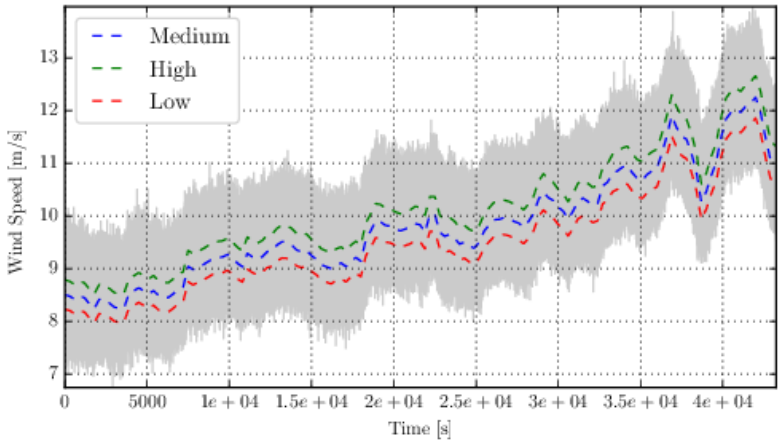

Figure 9: 5-minute scheduling – Trajectories of wind speeds for 12h. Dashed lines indicate the high, medium and low scenarios, respectively, while grey line indicate the same scenarios with inclusion of volatility.

3.2.1. Impact of different sSCUC strategies on power system dynamics

This section perform the same sensitivity analysis that is carried out for the 15-minute scheduling. Table 4 show the relevant results of such an analysis. A

Table 4: 5-minute scheduling – σ_{COI} for different sSCUC probabilities with $j = 3.333\%$.

Scenario	sSCUC	MC – TDS	σ_{COI} (10^{-4})
1	20% 60% 20%	20% 60% 20%	5.45
2	40% 50% 10%	20% 60% 20%	5.51
3	100% 0% 0%	20% 60% 20%	5.44
4	0% 100% 0%	20% 60% 20%	5.70
5	0% 0% 100%	20% 60% 20%	5.48
6	0% 20% 80%	20% 60% 20%	5.53
7	0% 40% 60%	20% 60% 20%	5.55
8	0% 60% 40%	20% 60% 20%	5.55
9	0% 80% 20%	20% 60% 20%	5.59

reduction of the value of σ_{COI} is observed for all scenarios. This is due to the lower level of wind power uncertainty. In particular, if we compare scenarios 1, 3 and 5, respectively, we can see that the differences are less significant. It appears that, if the uncertainty level is low and the system is scheduled more frequently, then differences between SCUC and sSCUC becomes less evident. This result can be explained by the fact that, even if there is an error in the forecast, the machines and the relevant controls will easily account for it. Therefore, if shorter interval of sSCUC are used and the system is scheduled more frequently, like, for example, in Australia [8], then system operators can still rely on deterministic approaches without compromising the dynamic performance of the system.

While the sensitivity analysis in case of the perfect forecast is shown in Table 5. The deterministic case with low wind gives the better dynamic behaviour, thus confirming the conclusions drawn for the 15-minute sSCUC.

Table 5: 5-minute scheduling – σ_{COI} for different sSCUC probabilities with $j = 3.333\%$.

Scenario	sSCUC	MC – TDS	σ_{COI} (10^{-4})
1	0% 0% 100%	0% 0% 100%	5.46
2	0% 100% 0%	0% 100% 0%	3.38
3	100% 0% 0%	100% 0% 0%	2.43

3.2.2. Impact of sSCUC wind uncertainty on power system dynamics

This section focus on the impact of wind power uncertainty on power system dynamics using a 5-minute scheduling. Similar to the 15-minute case, the wind power uncertainty level is increased from $j = 10\%$ to $j = 40\%$ with a step of 10%.

Figure 10 shows σ_{COI} as a function of wind power uncertainty. Again, we can see that such a relationship is almost linear within the used range. This suggests that, even using shorter sSCUC timescales, e.g. 5 minute, higher shares of RES will likely affect the dynamic performance of the system.

3.2.3. Impact of sSCUC wind volatility on power system dynamics

Following the same procedure as in the 15-minute case study, the standard deviation of wind power scenarios is increased from 10% to 40% with a step of 10%. Then, Fig. 10 shows σ_{COI} as a function of wind power volatility. This relationship is almost linear within the considered range, and so these findings just support the conclusions made above. Finally, the impact of wind power volatility on costs is shown in Fig. 11. Results indicate that the higher the wind power volatility, the higher the cost due to more ramping of generating units.

3.3. Impact of contingency on the transient response of the system using sSCUC and SCUC

In this section, we discuss whether a contingency leads to different dynamic behaviour of the system if using a sSCUC or SCUC. With this aim, the com-

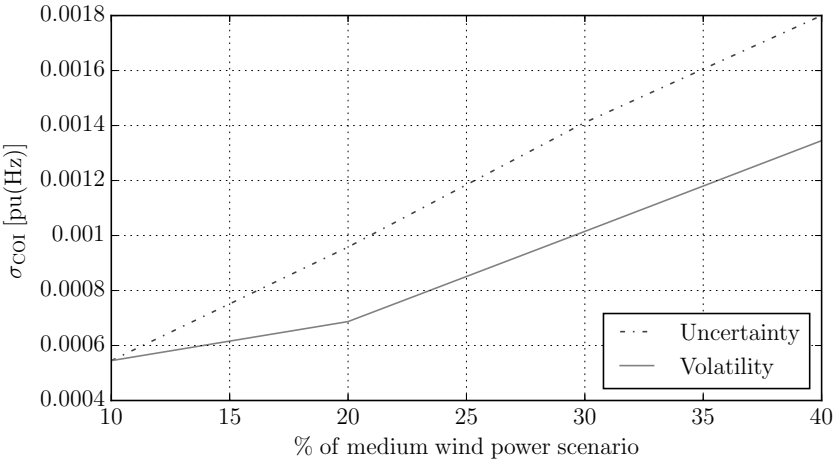

Figure 10: 5-minute scheduling – σ_{COI} as a function of wind uncertainty and volatility.

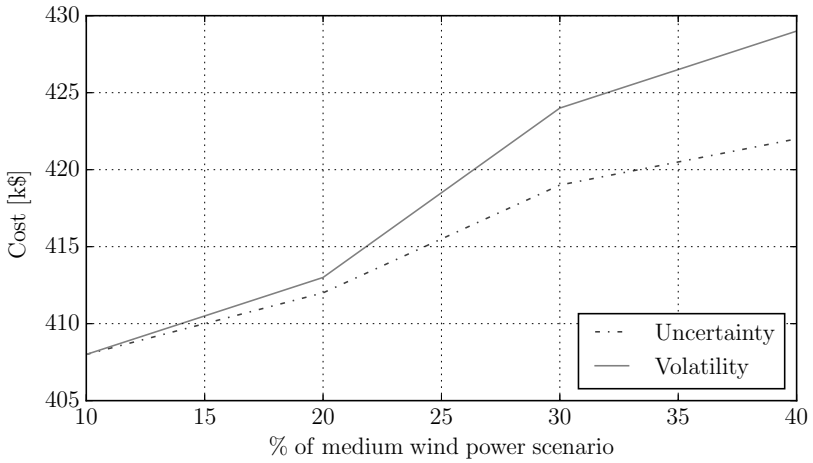

Figure 11: 5-min scheduling – Expected cost as a function of wind uncertainty and volatility.

parison is performed using scenario 1 (stochastic) and scenario 5 (deterministic) from Table 1.

A three-phase fault is applied at $t = 900$ s and cleared after 200 ms by disconnecting line 1. The impact of the contingency is shown in Figs. 12 and 13. Specifically, Fig. 12 depicts the trajectories of the rotor speed of the relevant machines during the contingency when using a sSCUC. Similarly, Fig. 13

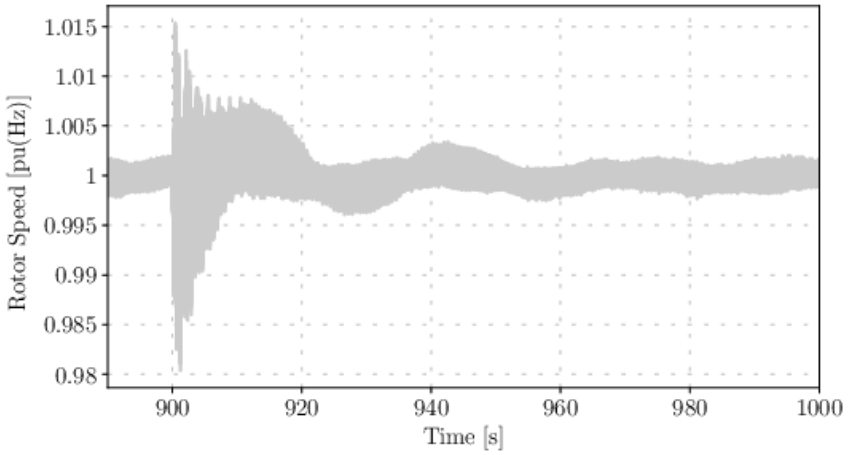

Figure 12: sSCUC and 25% wind penetration – Trajectories of the rotor speed of relevant machines following a contingency.

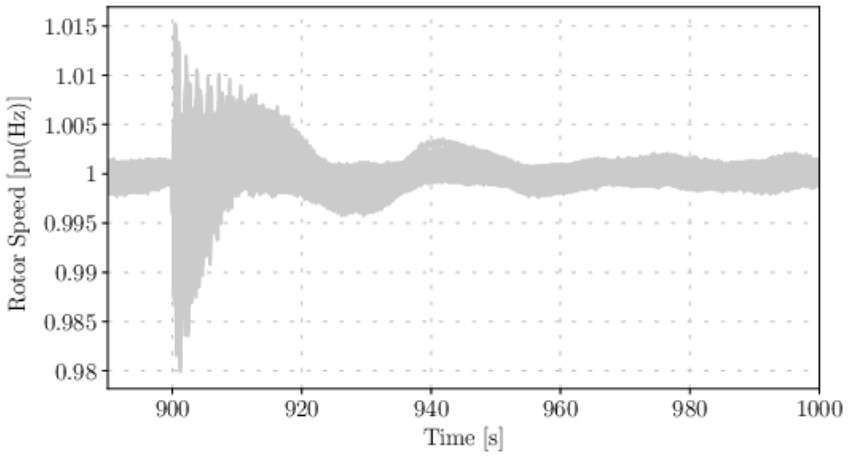

Figure 13: SCUC and 25% wind penetration – Trajectories of the rotor speed of relevant machines following a contingency.

depicts the trajectories of the rotor speed of the relevant machines during the contingency when using a SCUC. Results indicate that for the considered case study the impact of contingency is almost identical. This is due to the fact that the generator schedules obtained with the sSCUC and SCUC do not differ

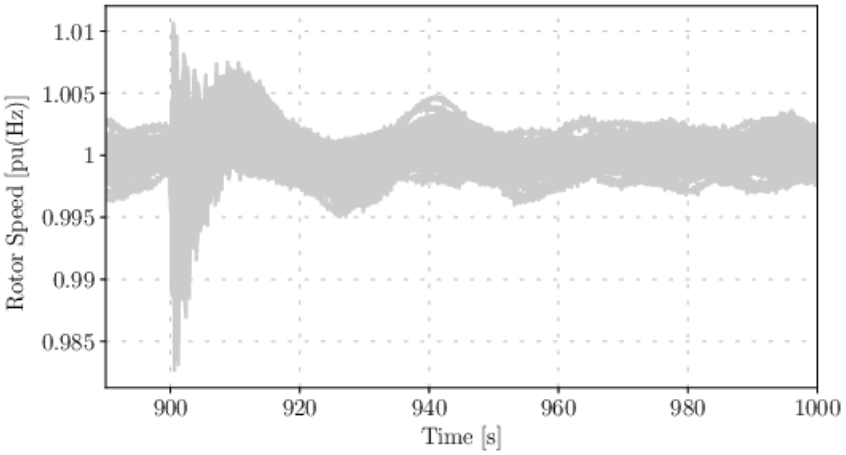

Figure 14: sSCUC and 50% wind penetration – Trajectories of the rotor speed of relevant machines following a contingency.

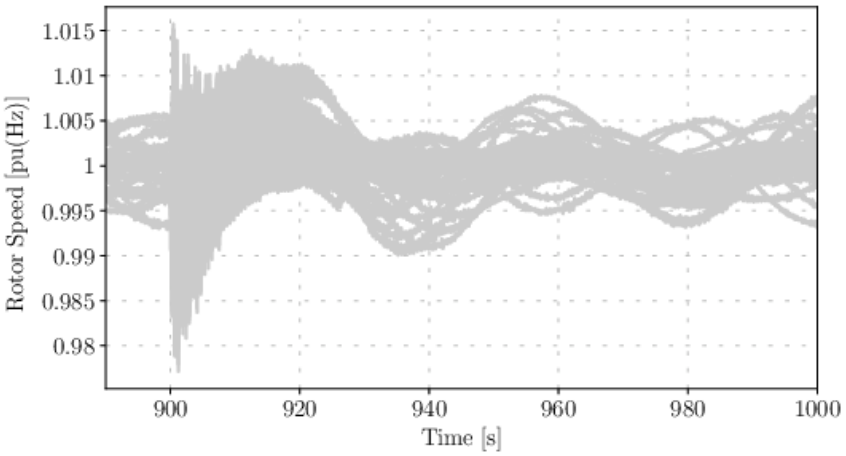

Figure 15: SCUC and 50% wind penetration – Trajectories of the rotor speed of relevant machines following a contingency.

significantly.

The same contingency is applied for the case of 50% wind penetration. Figures 14 and 15 show the trajectories of the rotor speed of the relevant machines during the contingency when using a sSCUC and SCUC, respectively. In this

case, the sSCUC leads to a better transient response of the system following a contingency. It appears that, one cannot know *a priori* which strategies of sSCUC are better from the dynamic viewpoint of the system before solving both sSCUC and SCUC problems.

3.4. Impact of renewable penetration on long-term frequency deviations using different sSCUC strategies

Increasing the penetration levels of RES changes the stability and dynamic performance of the system as well as makes real-time system operation more difficult for TSOs [2]. In this context, this section focuses on the impact of high penetration levels of RES, namely 50%, on the long-term frequency deviations using different sSCUC strategies. With this aim, and similar to Subsection 3.1.1, a sensitivity analysis with respect to different sSCUC probabilities for the low, medium and high wind power scenario is carried out.

Table 6 shows some relevant results of the analysis. There is a significant increase in the value of σ_{COI} in all scenarios compared to the case of 25% of wind penetration. This is to be expected as fewer synchronous generators that provide frequency regulation (primary and secondary) are now scheduled to be online and more power is being produced by stochastic sources.

It is interesting to note that the deterministic scenario with high wind power (scenario 5) is the worst with $\sigma_{\mathrm{COI}} = 0.002618$. Scenario 5, in fact, schedules fewer synchronous generators to be online compared to the same scenario in Section 3.1.1. In other words, there is less frequency regulation available online to cope with wind power uncertainty. Therefore, depending on the level of wind power uncertainty, as well as wind penetration level, TSOs can solve a sSCUC or SCUC with high wind. Specifically, according to our results, for low wind power uncertainty ($j < 30\%$) and 25% wind penetration level, it is better to solve a SCUC with high wind power. On the other hand, if the wind penetration level is 50% then TSOs can solve a sSCUC and/or SCUC with medium and low wind power, respectively.

Table 6: 15-minute scheduling – σ_{COI} for different sSCUC probabilities with $j = 10\%$ and 50% wind penetration.

Scenario	sSCUC	MC − TDS	σ_{COI} (10^{-4})
1	20% 60% 20%	20% 60% 20%	19.03
2	40% 50% 10%	20% 60% 20%	18.95
3	100% 0% 0%	20% 60% 20%	19.09
4	0% 100% 0%	20% 60% 20%	19.09
5	0% 0% 100%	20% 60% 20%	26.18

3.5. Impact of the number of sSCUC wind scenarios on the dynamic response of the system

In this section, we compare the impact of the number of sSCUC wind scenarios on the dynamic behaviour of power system. The comparison is performed using a 15 minute scheduling time period and 25% wind penetration. With this aim, we consider 10 wind power scenarios and perform a sensitivity analysis similar to Subsection 3.1.1. Wind power scenarios are built according to the wind maximum variation width j (see Fig. 1). In order to compare the results, a base-case scenario is considered with the following properties: sSCUC probabilities for the 10 scenarios (starting from low to high wind) are set as follows: 5%, 5%, 10%, 10%, 30%, 10%, 10%, 10%, 5%, 5%. Similarly, when we run the MC-TDS, the system is assumed to be with the folowing probabilities: 5%, 5%, 10%, 10%, 30%, 10%, 10%, 10%, 5%, 5%, starting from low to high wind scenario, respectively.

Figure 16 shows the trajectories of ω_{COI} for this base case scenario. Compared to Fig. 4 (3 sSCUC wind power scenarios), there is no significant difference in the dynamic behaviour of the system. To further support this, Table 7 shows some of the relevant results of the sensitivity analysis. As it can be seen, the long-term frequency deviations are similar to those in Table 1 and do not differ

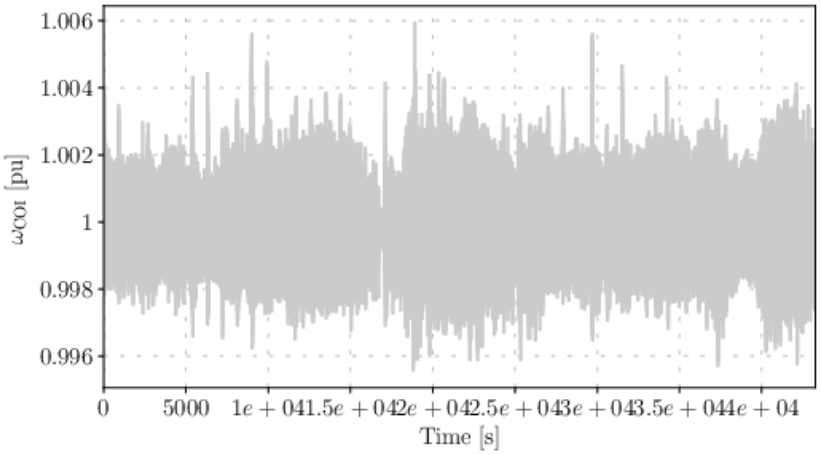

Figure 16: 15-minute scheduling – Trajectories of ω_{COI} for 10 sSCUC wind power scenarios.

Table 7: 15-minute scheduling – σ_{COI} for different sSCUC probabilities with $j = 10\%$ and 10 wind power scenarios.

Scenario	sSCUC	MC – TDS	σ_{COI} (10^{-4})
1	5%, 5%, 10%, 10%, 30%, 10%, 10%, 10%, 5%, 5%	5%, 5%, 10%, 10%, 30%, 10%, 10%, 10%, 5%, 5%	8.74
2	20%, 5%, 5%, 10%, 10%, 5%, 10%, 10%, 5%, 20%	5%, 5%, 10%, 10%, 30%, 10%, 10%, 10%, 5%, 5%	8.77
3	100%, 0%, 0%, 0%, 0%, 0%, 0%, 0%, 0%, 0%	5%, 5%, 10%, 10%, 30%, 10%, 10%, 10%, 5%, 5%	8.82
4	0%, 0%, 0%, 0%, 100%, 0%, 0%, 0%, 0%, 0%	5%, 5%, 10%, 10%, 30%, 10%, 10%, 10%, 5%, 5%	8.99
5	0%, 0%, 0%, 0%, 0%, 0%, 0%, 0%, 0%, 100%	5%, 5%, 10%, 10%, 30%, 10%, 10%, 10%, 5%, 5%	8.90

sigificantly between scenarios. It appears that, for the considered case, increasing the number of sSCUC wind power scenarios from 3 to 10 does not have a significant impact on the dynamic response of the system. Furthermore, these results support the above conclusion that a highly sophisitcated sSCUC might not be necessary if the scheduling is repeated with a short period.

3.6. Remarks and Recommendations

The results obtained in the case studies can be grouped in two categories, namely, as expected and less expected.

3.6.1. As expected

- Simulation results show that there exist a relationship between sSCUC intervals and frequency deviations. Shortening the sSCUC interval, e.g. from 15 to 5 minutes, leads to lower frequency fluctuations. These findings are in line with the results that were observed in real-world power systems [43].

- In case of perfect forecasts, simulation results show that the scenario with low wind gives a better dynamic behaviour compared to the medium and high wind power scenario.

- All simulation results show an almost linear relationship between sSCUC wind uncertainty and volatility and frequency variations. This means that as the penetration of RES increases, i.e., higher wind uncertainty and volatility, it will be more and more difficult for TSOs to manage the real-time balance between generation and demand. Therefore, there is a clear need for linear increase of the spinning reserves. Actually, these results support the idea that in systems with high RES penetration, e.g. Denmark and Ireland, the main concern for TSOs will be on how to cope with high ramp-up and ramp-down of RES rather than the traditional $N-1$ contingency criteria.

- In general, higher RES penetration leads to lower costs. However, simulation results indicate that while the total operating cost will be reduced, the reward of ancillary services will increase due to more ramping of generating units.

- Increasing the number of sSCUC wind power scenarios, namely, from 3 to 10, leads to very similar long-term frequency deviations of the system.

3.6.2. Less expected

- Different sSCUC strategies leads to very similar long-term dynamic behaviour of the system.

- For low wind uncertainty ($j < 30\%$) and 25% wind penetration level, solving a SCUC with high wind gives a better dynamic behaviour. Nevertheless, as uncertainty increases, it is recommended that a sSCUC should be used. When the wind penetration level is 50% then it is better to solve a sSCUC and/or SCUC with medium and low wind power, respectively. Moreover, when shortening the sSCUC interval and scheduling the system more frequently, the differences between these strategies are negligible. This is an important information for system operators since they still rely on deterministic approaches. Therefore, depending on the level of wind penetration and uncertainty, they can solve a SCUC without compromising the dynamic behaviour of power systems.

- According to our results, in case of 25% wind penetration, there is no significant difference on the transient response of the system following a contingency when using a sSCUC or SCUC. However, when increasing the wind penetration to 50% then a sSCUC leads to a better transient response of the system. Note that the 50% penetration is not a fixed threshold but depends on the considered grid, generator bids and available wind generation.

- Finally, results show that wind power uncertainty has a greater impact than volatility on the dynamic performance of the system, while the other way round is true for the impact on the expected cost.

4. Conclusions

This paper analyses the impact of the sub-hourly UC problem on power system dynamics. More specifically, the paper focuses on the impact of different strategies of sSCUC as well as different wind uncertainty and volatility scenarios included in the sSCUC on frequency variations. With this aim, a sub-hourly sSCUC is used to capture wind variability, while the uncertainty is captured through a stochastic sSCUC. Then, the sub-hourly sSCUC is embedded into a

time domain simulator (TDS), and a rolling approach is used to account for wind and load forecast updates. Embedding the UC problem into a TDS provides an useful simulation tool for TSOs in order to understand the impact interactions of UCs models with the actual dynamic response of the grid.

Simulation results based on MC-TDS show that there is no significant difference on long-term frequency deviations of the system when using different sSCUC strategies. Results also suggest that for low wind uncertainty, and 25% wind penetration level, system operators may want to solve a SCUC with high wind. However, as the sSCUC wind uncertainty increases then a sSCUC approach is to be preferred. In addition, in case the system is scheduled more frequently, then differences between stochastic and deterministic approaches becomes less evident. Regarding the impact of sSCUC wind scenarios, the case study shows that, increasing the number scenarios does not lead to any significant difference in the long-term frequency deviations. Furthermore, results show that sSCUC wind power uncertainty has a greater impact than volatility on the dynamic behaviour of the system.

The case studies show an almost linear relationship between higher sSCUC wind uncertainty and volatility, and higher frequency variations. From a TSO point of view, this means a challenge for future operation as the penetration of RES is expected to increase. Hence, the safe integration of RES indicate a need for linear increased ancillary services (spinning reserves) in order to ensure a reliable operation of power systems.

Results suggest that for 25% wind penetration, both sSCUC and SCUC leads to almost identical transient response of the system following a contingency. On one hand, sSCUC leads to a better transient response of the system in case of 50% wind penetration. On the other hand, when the wind penetration level reaches 50%, solving a sSCUC and/or SCUC with medium and low wind power, respectively, leads to lower long-term frequency deviations of the system.

Future work will focus on designing a feedback control that will take a signal from the system and send it to the sSCUC. Other works will also consider the interaction between sSCUC, microgrids and DAEs. Finally, a study on the

impact of sub-hourly UC with inclusion of voltage constraints on long-term dynamic behaviour of the system will be considered.

Acknowledgements

This work was supported by Science Foundation Ireland, by funding T. Kërçi and F. Milano under project ESIPP, Grant No. SFI/15/SPP/E3125; F. Milano under project AMPSAS, Grant No. SFI/15/IA/3074; and J. S. Giraldo under the Coordenação de Aperfeiçoamento de Pessoal de Nível Superior, Brazil (CAPES), Finance Code 001.

Bibliography

References

[1] Y. Fu, M. Shahidehpour, Z. Li, Security-constrained unit commitment with ac constraints, IEEE Trans. on Power Systems 20 (3) (2005) 1538–1550.

[2] CIGRE and CIRED, Modelling of inverter-based generation for power system dynamic studies.

[3] F. Milano, F. Dörfler, G. Hug, D. J. Hill, G. Verbič, Foundations and challenges of low-inertia systems (invited paper), in: Power Systems Computation Conference (PSCC), 2018, pp. 1–25.

[4] A. Conejo, M. Carrión, J. Morales, Decision Making Under Uncertainty in Electricity Markets, Springer, 2010.

[5] A. Tuohy, P. Meibom, E. Denny, M. O'Malley, Unit commitment for systems with significant wind penetration, IEEE Trans. on Power Systems 24 (2) (2009) 592–601.

[6] F. Bouffard, F. D. Galiana, Stochastic security for operations planning with significant wind power generation, IEEE Trans. on Power Systems 23 (2) (2008) 306–316.

[7] ENTSO-E, An Overview of the European Balancing Market and Electricity Balancing Guideline, Nov 2018.

[8] I. MacGill, Electricity market design for facilitating the integration of wind energy: Experience and prospects with the australian national electricity market, Energy Policy 38 (7) (2010) 3180 – 3191.

[9] Nord Pool, Nord Pool key statistics – March 2019.
URL https://www.nordpoolgroup.com

[10] European Commission, Commission Regulation (EU) 2017/2195 of 23 November 2017 establishing a guideline on electricity balancing (2016).

[11] AEMO, Australian energy market operator.
URL https://www.aemo.com.au/

[12] E. Hillberg, A. Zegers, B. Herndler, S. Wong, J. Pompee, J.-Y. Bourmaud, S. Lehnhoff, G. Migliavacca, K. Uhlen, I. Oleinikova, et al., Flexibility needs in the future power system.

[13] I. D. López, D. Flynn, M. Desmartin, M. Saguan, T. Hinchliffe, Drivers for sub-hourly scheduling in unit commitment models, in: IEEE PES General Meeting, 2018, pp. 1–5.

[14] J. P. Deane, G. Drayton, B. Ó Gallachóir, The impact of sub-hourly modelling in power systems with significant levels of renewable generation, Applied Energy 113 (2014) 152 – 158.

[15] H. Gangammanavar, S. Sen, V. M. Zavala, Stochastic optimization of sub-hourly economic dispatch with wind energy, IEEE Trans. on Power Systems 31 (2) (2016) 949–959.

[16] N. Troy, D. Flynn, M. O'Malley, The importance of sub-hourly modeling with a high penetration of wind generation, in: IEEE PES General Meeting, 2012, pp. 1–6.

[17] P. Kundur, J. Paserba, V. Ajjarapu, G. Andersson, A. Bose, C. Cañizares, N. Hatziargyriou, D. Hill, A. Stankovic, C. Taylor, T. Van Cutsem, V. Vittal, Definition and classification of power system stability IEEE/CIGRE joint task force on stability terms and definitions, IEEE Trans. on Power Systems 19 (3) (2004) 1387–1401.

[18] T. Kërçi, F. Milano, A framework to embed the unit commitment problem into time domain simulations, in: EEEIC, Genoa, Italy, 2019, pp. 1–5.

[19] T. Kërçi, F. Milano, Sensitivity analysis of the interaction between power system dynamics and unit commitment, in: 2019 IEEE PowerTech, Milan, Italy, 2019, pp. 1–6.

[20] P. Daly, H. W. Qazi, D. Flynn, Rocof-constrained scheduling incorporating non-synchronous residential demand response, IEEE Trans. on Power Systems (2019) 3372–3383.

[21] H. Ahmadi, H. Ghasemi, Security-constrained unit commitment with linearized system frequency limit constraints, IEEE Trans. on Power Systems 29 (4) (2014) 1536–1545.

[22] M. Paturet, U. Markovic, S. Delikaraoglou, E. Vrettos, P. Aristidou, G. Hug, Stochastic unit commitment in low-inertia grids, arXiv preprint arXiv:1904.03030.

[23] P. Vorobev, D. M. Greenwood, J. H. Bell, J. W. Bialek, P. C. Taylor, K. Turitsyn, Deadbands, droop, and inertia impact on power system frequency distribution, IEEE Trans. on Power Systems 34 (4) (2019) 3098–3108.

[24] ENTSO-E, Continental europe significant frequency deviations – January 2019.

[25] S. Chatzivasileiadis, M. Bonvini, J. Matanza, R. Yin, T. S. Nouidui, E. C. Kara, R. Parmar, D. Lorenzetti, M. Wetter, S. Kiliccote,

Cyber–physical modeling of distributed resources for distribution system operations, Proceedings of the IEEE 104 (4) (2016) 789–806. doi:10.1109/JPROC.2016.2520738.

[26] P. Palensky, A. A. Van Der Meer, C. D. Lopez, A. Joseph, K. Pan, Cosimulation of intelligent power systems: Fundamentals, software architecture, numerics, and coupling, IEEE Industrial Electronics Magazine 11 (1) (2017) 34–50. doi:10.1109/MIE.2016.2639825.

[27] P. Palensky, A. van der Meer, C. Lopez, A. Joseph, K. Pan, Applied cosimulation of intelligent power systems: Implementing hybrid simulators for complex power systems, IEEE Industrial Electronics Magazine 11 (2) (2017) 6–21.

[28] K. Hopkinson, Xiaoru Wang, R. Giovanini, J. Thorp, K. Birman, D. Coury, Epochs: a platform for agent-based electric power and communication simulation built from commercial off-the-shelf components, IEEE Transactions on Power Systems 21 (2) (2006) 548–558. doi:10.1109/TPWRS.2006.873129.

[29] F. Plumier, P. Aristidou, C. Geuzaine, T. Van Cutsem, Co-simulation of electromagnetic transients and phasor models: A relaxation approach, IEEE Transactions on Power Delivery 31 (5) (2016) 2360–2369. doi:10.1109/TPWRD.2016.2537927.

[30] F. Milano, R. Zárate-Miñano, A systematic method to model power systems as stochastic differential algebraic equations, IEEE Trans. on Power Systems 28 (4) (2013) 4537–4544.

[31] F. Milano, Power System Modelling and Scripting, Springer, London, 2010.

[32] IEA-WIND, Design and operation of power systems with large amounts of wind power.

[33] I. Blanco, J. M. Morales, An efficient robust solution to the two-stage stochastic unit commitment problem, IEEE Trans. on Power Systems 32 (6) (2017) 4477–4488.

[34] J. M. Morales, A. J. Conejo, J. Perez-Ruiz, Economic valuation of reserves in power systems with high penetration of wind power, in: IEEE PES General Meeting, 2009, pp. 1–1.

[35] EirGrid Group, System and Renewable Data.
URL http://www.eirgridgroup.com/how-the-grid-works/renewables/

[36] J. Wang, M. Shahidehpour, Z. Li, Security-constrained unit commitment with volatile wind power generation, IEEE Trans. on Power Systems 23 (3) (2008) 1319–1327.

[37] F. Milano, A Python-based software tool for power system analysis, in: IEEE PES General Meeting, Vancouver, BC, 2013, pp. 1–5.

[38] A. Gómez Expósito, A. J. Conejo, C. Cañizares, Electric energy systems: analysis and operation, CRC press, 2018.

[39] M. Costley, M. J. Feizollahi, S. Ahmed, S. Grijalva, A rolling-horizon unit commitment framework with flexible periodicity, I. J. of Electrical Power & Energy Systems 90 (2017) 280 – 291.

[40] Illinois Center for a Smarter Electric Grid (ICSEG), IEEE 39-Bus System, URL: http://publish.illinois.edu/smartergrid/ieee-39-bus-system/.

[41] M. Carrión, J. M. Arroyo, A computationally efficient mixed-integer linear formulation for the thermal unit commitment problem, IEEE Trans. on Power Systems 21 (3) (2006) 1371–1378.

[42] L. Gurobi Optimization, Gurobi optimizer reference manual (2018).
URL http://www.gurobi.com

[43] B. Schafer, M. Timme, D. Witthaut, Isolating the impact of trading on grid frequency fluctuations, in: IEEE ISGT-Europe, 2018, pp. 1–5.